BioMetals **13:** 169–178, 2000.

Voltage-clamp: a useful approach to study *in vitro* duodenal iron transport in the mouse

Luciana M.G. Costa[1,2,3], Augusta Rebelo da Costa[2,3] & Maria de Sousa[2,3,*]
[1]*Departmento de Química, Centro de Química Fina e Biotecnologia, Faculdade de Ciências e Tecnologia, Universidade Nova de Lisboa, 2825 Monte da Caparica, Portugal*
[2]*Unidade de Imunologia Molecular, Instituto de Biologia Molecular e Celular, 4150 Porto, Portugal*
[3]*Instituto de Ciências Biomédicas de Abel Salazar, 4050 Porto, Portugal*
[*]*Author for correspondence (Tel: +351-22-6074955; Fax: +351-22-6098480; E-mail: mdesousa@ibmc.up.pt)*

Received 5 March 2000; accepted 5 April 2000

Key words: duodenum, iron absorption, mouse, ussing-chamber

Abstract

The mechanism(s) controlling iron absorption remain(s) uncertain despite the progress in the identification of genes selectively expressed in the duodenum. The availability of experimental models of iron absorption is critical to the clarification of such mechanism(s). In the present study, a simple method for studying *in vitro* iron absorption in mouse duodenum is described. Short circuit current, open circuit potentials and epithelial conductances were measured in mouse duodenal segments. Also, unidirectional ^{55}Fe fluxes at different pH conditions were measured in mice with varying iron status. The findings reinforce evidence for an adaptive response of the iron absorptive process according to the body iron status. Significant differences are demonstrated between iron fluxes measured in normal and parenterally iron loaded mice and at acidic compared to neutral pH environment. Also, a significant difference was observed between transepithelial potential measured in duodenum from iron-loaded compared to untreated mice. Advances in the understanding of the mechanism(s) of iron absorption can be brought by the application of voltage-clamp techniques to the electrophysiologic study of iron overload mouse models.

Introduction

The control of iron absorption in humans is a carefully regulated biological mechanism that responds rapidly to alterations in body iron status by an appropriate increase or decrease in the uptake of iron from the intestinal lumen (Conrad *et al.* 1963; Crosby *et al.* 1963; Halliday 1992). The biochemical and physiologic processes involved in this regulation have not been fully clarified.

The understanding of the function of transporting epithelia has been advanced by the introduction of model systems to study permeability and electric properties *in vitro* (Alvarez-Hernandez *et al.* 1992; Ferreira *et al.* 1992, Hegel *et al.* 1993, Sugawara *et al.* 1995). Also, vectorial transport of ions and small molecules across the epithelial cell cytoplasm requires that opposite sides of the plasma membranes (mucosal and serosal aspects) be endowed with different specialized biochemical properties. The short-circuit current experiment introduced for over 40 years ago (Ussing & Zerahn 1951) has been used previously to study ion transport in small intestine of various species (Schultz & Zalusky 1964a, b; Okada *et al.* 1975, 1976; Madsen *et al.* 1996). However, despite intense research in mouse and rat intestinal electrolyte transport by measuring electrical parameters (Raja *et al.* 1989; O'Riordan *et al.* 1995a, b) no Ussing-type model of the mouse duodenum in which specific transport systems are allocated to the two cell-barriers has been tested until now.

In the last two years several new genes involved in iron metabolism have been identified, cloned and characterized (Fleming *et al.* 1997; Gushin *et al.* 1997; Feder *et al.* 1996). The specific roles of the different components involved have been assessed by identi-

fying mutations in relevant genes related to human diseases or by generating and phenotyping genetically altered mice (Fleming *et al.* 1998; Zhou *et al.* 1998; Bahram *et al.* 1999).

Given the importance of the murine models to study iron metabolism (Edwards *et al.* 1970; De Sousa *et al.* 1994; Santos *et al.* 1996) this report describes a new and convenient method for the physiologic characterization and iron transport in mouse duodenum.

The present work was carried out to test the validity of radionuclide uptake and flux techniques in short circuit conditions to study vectorial iron movement across mouse duodenum. The *in vitro* method described reproduces the results of the adaptive responses to changes in body iron requirements obtained *in vivo* and provides a useful tool for the characterization of the electrophysiology of mouse duodenum. Also, the data obtained indicate a putative influence of iron loading in the transepitelial potential measured in mouse duodenum.

These results support the use of this Ussing-type model to gain insight into the mechanisms involved on the regulation of iron absorption.

Materials and methods

Animals and housing

C57BL/6 (B6) male mice aged 6–8 weeks were purchased from a local supplier (IGC Oeiras, Portugal) and the Jackson ImmunoResearch Laboratories (West Grove, PA, USA). The mice were housed in groups not greater than 5 animals in wire-topped polycarbonate cages, with a layer of corncob, grade 12 as bedding material. Room lighting, temperature and humidity were kept controlled (14 h light/10 h dark cycle; 20–23 °C; 40%–60% humidity). Acid-treated water and a commercial rodent diet (Harlan Teklad Autoclavable diet 9605) were provided *ad libitum*. Clean cages with fresh bedding were introduced once a week.

Establishment of iron status

To induce parenteral iron loading, 5 mg of iron-dextran (Sigma Immunochemicals) was injected subcutanously. The mice were left two weeks before the experiments to allow for iron redistribution. Untreated mice were used as controls.

Measurement of liver iron levels

Iron concentration was determined in livers from parenterally over-loaded B6 mice (Fe+) and controls (FeN). Liver samples were digested by nitric acid p.a. and the ashes dissolved in chloridric acid p.a. Analytical measurements were made by Plasma Emission Spectroscopy (PES) on a Perkin Elmer 400 model.

Tissue handling

The animals were killed by cervical dislocation. The abdomen was quickly opened by a mid-line incision. The duodenum and part of jejunum was removed and carefully washed with oxygenated control solution at room temperature. A fire-polished glass rod 3mm in diameter was inserted to the lumen and the outer layers of the intestine were gently dissected out. The epithelium was cut longitudinally along the mesenteric border and pieces about 0.8 cm long apart from the pylorus were used for the chambers. This tissue corresponds to the proximal duodenum. Discs of adequate diameter were cut from acetate sheet and an oblong hole with an area of 0.32 cm^2 was punched into the center of each disc. The epithelium was glued to the rim of these holes with tissue adhesive (isobutyl-2-cyanoacrylate, Ethicon) and mounted in the appropriate Ussing-type chambers bathed on either side with 4 ml of the control solution (Marvão *et al.* 1994).

Solutions

The control buffer solution had the following composition: 120 mM NaCl, 5 mM KCl, 1 mM $CaCl_2$, 1 mM $MgSO_4$, 20 mM $NaHCO_3$, 10 mM D-Glucose. In ion substitution experiments, sodium was equimolary replaced by N-methyl-D-glucamine (NMG). In these solutions, the ionic calcium concentration was measured with a calcium electrode (Diamond Electro-Tech Inc.) and adjusted to 1 mM. All the ion replacements were bilateral. The solutions were kept at pH=7.4 (or 5.5 when specified) by bubbling with 95%O_2 plus 5%CO_2 saturated with water vapor. The osmolality of all solutions was 290 mosm/Kg water.

The following transport inhibitors were used: ouabain 1 mM (Sigma), 4,4-diisothiocyano-stilbene 2,2 disulphonic acid (DIDS) 0.5 mM (Sigma), amiloride 1 mM (Merk, Sharp & Dohme), furosemide 0.1 mM (Hoechst), picrylsulphonic acid (PSA) 0.5 mM (Sigma), acetazolamide (DIAMOX) 1 mM (Lederle) and diphenylamin-2-carboxylate (DPC)

1 mM (Aldrich, Steinheim). Concentrations given correspond to the final concentrations in the chamber. Inhibitors were always applied to only one side of the epithelium.

Transepithelial electrical measurements

For transepithelial measurements, preparations with an exposed area of 0.32 cm^2 were mounted in Ussing-type chambers and bathed with control solution. The lumen side of the epithelium will be called the mucosal (M) or apical side, while the opposite side will be called the serosal or the basolateral side (S).

Electrical continuity between the KCl-saturated solutions, where the current injecting electrodes (Ag/AgCl) and the voltage-measuring (calomel) electrodes were immersed, and the two half chambers was made through salt bridges of 3.5% agar in control solution. Calomel electrodes were manufactured in the laboratory and maintained short-circuited when not used. Before each experiment, calomel electrodes differing by less than 0.1 mV were selected, the chambers without the preparation were assembled and the resistance between the tips of the voltage bridges were measured for each chamber filled with control solution. This procedure enables the compensation for the electrical potencial drop between the tips of the voltage bridges and the preparation (Ferreira & Marshal 1985). The preparation was kept at room temperature and continuously short circuited by an automatic voltage-clamp system which compensated for control solution resistance. Total conductance was measured by displacing the transepithelial potential by 1 mV and measuring the corresponding deflection of the current. Experiments were performed only after steady-state was reached for at least 60 min.

Iron flux measurements

^{55}Fe was used as tracer for iron. Fe absorption was determined using ^{55}Fe(III) citrate added to Fe(II) as ferrous sulphate and a 20× molar excess of L-ascorbic acid solution. ^{55}Fe(III) citrate was prepared by addition of $^{55}FeCl_3$ (Amersham, UK) to a mixture of Na_3-citrate/Na_2CO_3 (3:2).

In order to study the influence of pH of the bath solution on the influx of iron, solutions at pH=7.4 or pH=5.5 (by addition of ascorbic acid) were used. The pH was kept stable by bubbling with 95%O_2 plus 5%CO_2 saturated with water vapor. In each experiment, the iron influx (mucosal to serosal side) was determined by adding the isotope to the apical side of the half-chambers bathed with the control solution. The concentration of iron in the apical side of the chamber at the beginning of the experiment was 7.2 μM.

The liquid in the unlabelled half chamber was collected into scintillation vials at 5, 10, 30, 60, 90 and 120 min after the addition of the isotope. A volume of 0.1 ml of the solution from the labeled side of each chamber was sampled at the beginning and the end of the experiment.^{55}Fe activity was measured by beta counting. The values were corrected for unspecific Fe-binding to the chambers and activity decay of the isotope during the experiments. All the fluxes are computed as the amount of radioactivity gathered in the collection period divided by the activity in an aliquot (0.1 ml) of the 'hot' solution.*

Study of the activity decay of ^{55}Fe during unidirectional iron flux experiments

Different protocols were used in order to clarify the nature of the isotope activity decay observed in the labeled solution added to the apical side during unidirectional iron flux experiments.

To test for a possible nonspecific binding of the isotope, assembled Ussing chambers without mounted duodenum were filled with labeled solution during the correspondent time interval of an usual unidirectional iron flux trial. After collection of the labeled solution for beta counting, the chambers were washed twice for 60 min with an unlabelled $FeSO_4$ 10 mM solution in order to release the ^{55}Fe possibly bound to the Perspex walls. The wash solutions were collected and radioactivity was measured. The 3.5% agar salt bridges were also removed and collected in different scintillation vials for beta counting.

In a separate set of experiments, the labeled solution added to the apical side during unidirectional iron flux experiments was periodically sampled in order to characterize the time course of the activity decay.

The data acquired from these experiments enable us to create an analysis model to correct for unspecific ^{55}Fe-binding to the Ussing chambers and activity decay during these trials (see Results).

Statistical analysis

Results are presented as means and standard errors of the mean (S.E.M.). All statistical tests were Student's

*If we define activity as the number of counts/unit time (measurement in the counter), the flux measurements are expressed as: (activity/time)/(activity/volume) = volume/time.

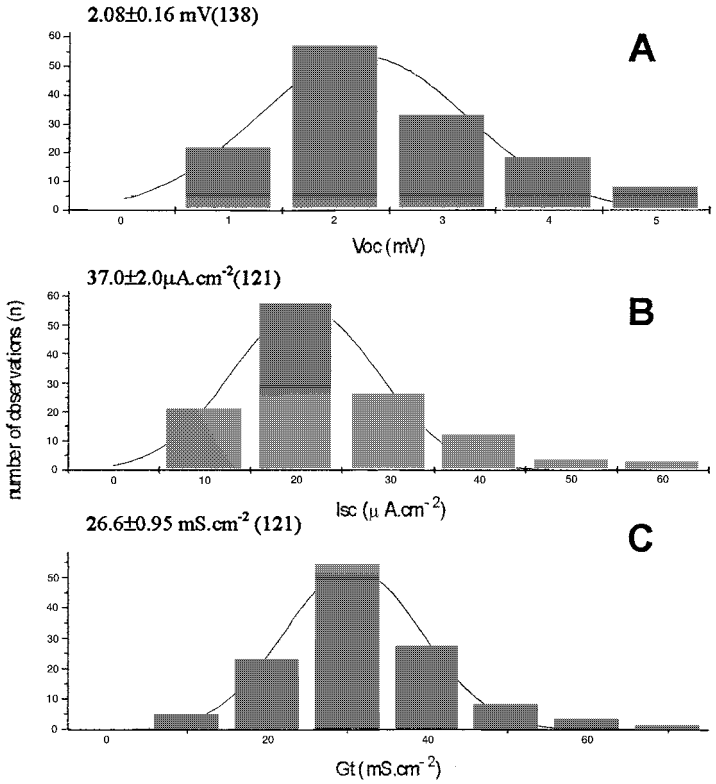

Figure 1. Histogram of transepithelial electrical parameters measured under control conditions in mice duodenum mounted in Ussing chambers. (A) open circuit potential (Voc) in mV; (B) short-circuit current (Isc) in μA.cm^{-2}; (C) total conductance (Gt) in mS.cm^{-2}. Mean values $\pm$ S.E.M. are given in the upper left-hand corner of each panel. Number of observations is given in parentheses.

t-tests. The hypothesis tested in each case was that the difference between two mean values was different from zero.

Results

Transepithelial electrical measurements

The duodenum is a single-layer epithelium which, when mounted *in vitro* under the conditions described in Materials and Methods generates a short circuit current (Isc) corresponding to the net flow of a positive charge towards the serosal side. After an initial transient period, the Isc decays slowly for at least 6 hours. In the same experimental conditions, the duodenum is able to generate a spontaneous and stable electrical potential difference (Voc) of 2.08$\pm$0.16 mV ($n = 138$, serosal side positive) (Figure 1A). For pooled results (Figure 1B), the measured Isc was 37.0$\pm$2.0 μAcm^{-2} ($n = 121$) and the electric conductance of the epithelium (Gt, Figure 1C) was 26.6$\pm$0.95 mScm^{-2} ($n = 121$).

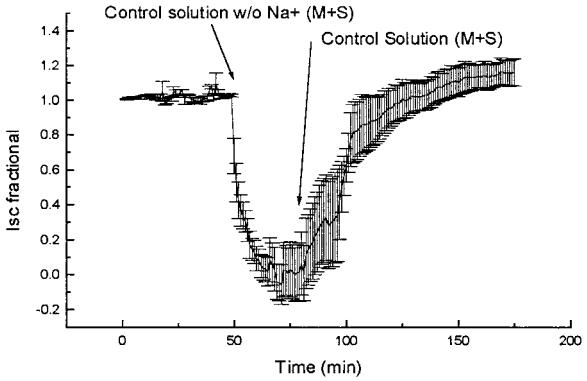

Figure 2. Time course of the effects on Isc caused by the bilateral (M+S) replacement of sodium by NMG (control solution w/o Na^+) in the external solution. The plotted current values are expressed as a fraction of the current measured at the moment when the first replacement was performed. Mean values are plotted and error bars correspond to the S.E.M, $n = 4$.

The frequency distribution curves of Isc, Voc and Gt show a unimodal distribution and, thus, seem to belong to a single population sample.

Table 1. Transepithelial electrical measurements made under control conditions in duodenum from untreated (FeN, $n = 8$) and parenterally iron-loaded (Fe+, $n = 7$) B6 mice. Data are presented as mean values ± S.E.M.

Transepithelial electrical measurements	FeN	Fe+
Isc (μA.cm^{-2})	26.6 ± 2.47	32.1 ± 5.22
Voc (mV)	2.51± 0.28[a]	1.4 ± 0.18[a]
Gt (mS.cm^{-2})	24.59 ± 2.14	26.8 ± 1.78

[a] $p<0.02$, comparison between untreated and iron-loaded B6 mice.

To analyze the nature of the Isc, its dependence on the ionic composition of the external solution was studied. The effect produced on Isc by the equimolary replacement of sodium by N-methyl-D-glucamine (NMG) in the control solution is shown in Figure 2. The first arrow in the graph indicates the time when the control solution from both half chambers (M + S) was substituted by NMG solution. As seen in the graph, the current was completely abolished when sodium was replaced by NMG in the external solution. In addition, the immediate current drop with an initial rate of 0.2 min^{-1} strongly suggests a direct involvement of the sodium ion in the current genesis. The second arrow in the graph points out the time of reintroduction of the control solution. The observedIsc recovery reconfirms the direct role of sodium on the current generation.

Effect of iron-loading on transepithelial electrical measurements

In order to investigate a possible effect of iron-loading on the transepithelial electrical properties of epithelium, short circuit current, electrical potential difference and electric conductance were measured in untreated (FeN, $n = 8$) and parenterally iron-loaded (Fe+, $n = 7$) B6 mice. The results show a significant difference between transepithelial potencial difference (Voc) measured in duodenum from iron-loaded mice compared to controls (Table 1).

Effect of transport inhibitors and Diamox on Isc

The values of Isc at any time were divided by the value at the time when the inhibitor was added (Isc fractional). The effects of the inhibitors where studied separately whenever the inhibitor was added to the mucosal side (M) or to the serosal side (S) (Figure 3).

Ouabain (1mM), a specific inhibitor of sodium pump Na^+/K^+ ATPase (Zeuthen 1992) produced an irreversible inhibition of the Isc when applied from the serosal side (Figure 3A) and was ineffective when applied from the mucosal side. In the graph, the arrow indicates the drug addition to the basolateral half chamber at a final concentration of 1 mM. The initial rate of current fall when ouabain was added to the serosal bath was 0.02 min^{-1} indicating thus, only an indirect effect on Isc. These findings are in agreement with the well-established theory that the exit-membrane for leaky epithelia is the exclusive location of Na^+/K^+ATPase. In this way, ouabain only inhibits Na^+ transport when applied to the exit side of the epithelium that is the basolateral membrane in the case of duodenum.

Picrylsulphonic acid, an inhibitor of the sodium-dependent bicarbonate/chloride antiport (Madsus & Olsnes 1987) when used at a final concentration of 0.5 mM was ineffective if applied from the mucosal side. However, it produced a 40% Isc increase when applied from the serosal side (Figure 3B). The arrow in the graph shows the time addition of the drug to the basolateral half chamber. The observed Isc raise had an initial rate constant of 0.004 min^{-1}. These results suggest picrylsulphonic acid has an indirect effect on the Isc probably caused by ionic gradient changes as a result of $Na^+/Cl^-/HCO_3^-$ antiport inhibition in the basolateral side of duodenum epithelium. DIDS, a well-studied inhibitor of the anionic shuttle (Cabantchik & Greger 1992, Gleeson 1992) was used on both sides of the preparation at a final concentration of 0.5 mM. As shown in Figure 3C, DIDS doubled the Isc when applied from the serosal side. However, Isc inhibition was observed if the drug was added to the mucosal bathed solution (Figure 3D). The effect caused by DIDS showed an initial rate constant of 0.08 min^{-1} and 0.04 min^{-1} respectively for serosal and for mucosal side application. Taken together these results suggest an indirect effect on Isc caused through alterations in the cell anionic shuttle process.

The effect produced on Isc when DPC at a final concentration of 1 mM was used in the mucosal or in the serosal side of duodenal mouse epithelium is shown in Figures 3E and 3F. Inhibition of the Isc was observed when the drug was applied either from the mucosal or serosal side. Seventy percent Isc inhibition was observed at an initial rate constant of 0.02 min^{-1} after DPC addition from the apical side of duodenum whereas 50% Isc inhibition at an initial rate constant of 0.01 min^{-1} was a result from DPC application in

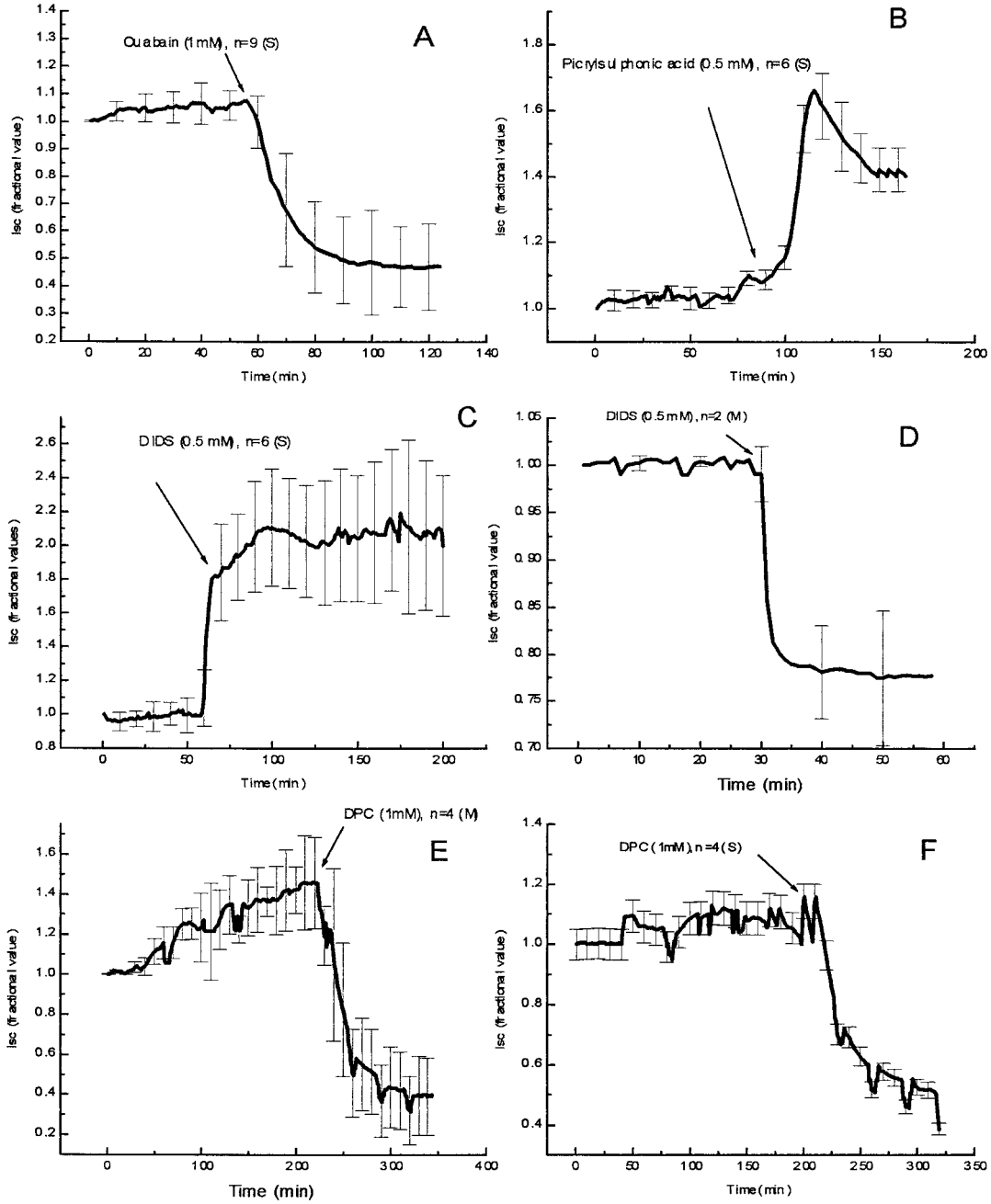

Figure 3. Time course of the effects of a group of transport inhibitors on Isc. Plotted current values are expressed as a fraction of the current measured at the moment when the inhibitor was added. Continuous lines correspond to the mean values of the number of experiments. Error bars give the S.E.M. The final concentration of the inhibitor is given between parentheses.

the opposite side. These findings indicate an indirect influence of DPC in the current and suggests the existence of DPC-sensitive chloride channels on both sides of epithelium (Stutts *et al.* 1990).

Amiloride (1 mM), Furosemide (0.1 M) and Diamox (1 mM) were ineffective when applied from either side of the epithelium.

Unidirectional iron flux measurements

Preliminary unidirectional (mucosal-to-serosal) iron flux experiments show an appreciable decrease with time in activity of the labeled solution added to the apical side. Two processes could explain this decay:
(a) Isotope accumulation in the intestinal tissue.
(b) Isotope transfer to the basolateral medium ('cold side').

However, the sum of the total radioactivity measured in the tissue and transferred to the 'cold' medium could not explain the fall in activity observed in the 'hot' solution. ^{55}Fe uptake studies done at pH=7.4 (n=4) and pH=5.5 (n=4) showed the radioactivity measured in duodenum from B6 mice could only account for a small proportion of the total activity measured in the apical side solution (0.18%±0.04 and 2.18%±0.48, respectively). In order to understand the activity decay observed in the 'hot' apical solution, ^{55}Fe adsorption to the chamber was tested. Ussing chambers without biological preparation were filled with 'hot' solution during the estimate time for a typical iron flux experiment. After collection of the 'hot' solution the chambers were washed twice with a 10 mM $FeSO_4$ solution for 60 min. All the wash solutions were collected and kept for radioactivity measurement. Also, the salt bridges were carefully removed and the radioactivity measured. The results obtained from these experiments show the existence of isotope binding to the chamber Perspex walls and to the 3.5% agar salt bridges (Figure 4). This binding proved to be very strong since the wash with the cold solution did not remove the total bound radioisotope.

Further studies of unidirectional iron flux experiments in which the labeled solution added to the apical side was periodically measured for ^{55}Fe radioactivity demonstrate that the isotope activity decay is an exponential process with a time constant around 20 min (Figure 5). The graph shows the ratio between the radioactivity measured and the radioactivity calculated assuming an exponential decay according to the formula:

$$\mathrm{Hf} + (\mathrm{Hi} - \mathrm{Hf})\mathrm{e}^{-\mathrm{Kt}},$$

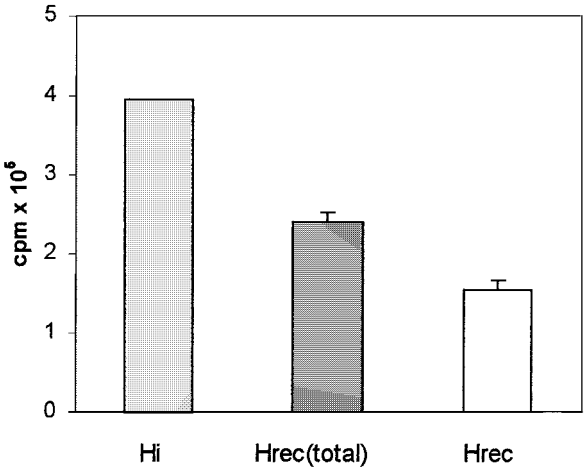

Figure 4. Radioactivity recovered from Ussing-chambers after wash with unlabeled saturated $FeSO_4$ solution and collection of agar salt bridges at the end of the experiment. Hi (radioactivity measured on the labeled solution in the beginning of the experiment); Hrec (total) (sum of the radioactivity measured on the solution collected at the end of the experiment, the wash solutions 1 h and 2 h after the end of the experiment and the salt bridges); Hrec (sum of the radioactivity measured on wash solutions 1 h and 2 h after the end of the experiment and the salt bridges). Values correspond to means ± S.E.M. of $n = 2$ experiments.

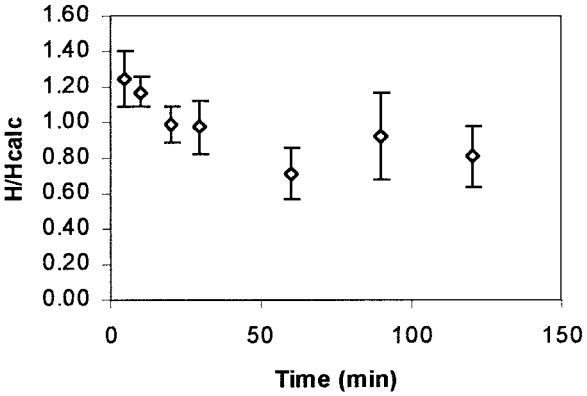

Figure 5. Study of the activity exponential decay observed in the labeled apical solution during unidirectional iron flux experiments. Values on the graph represents the ratio between the radioactivity periodically measured in the labeled apical solution (H) and the calculated values assuming the existence of an exponential decay process (Hcalc). The values are given as mean±S.E.M., $n = 6$ experiments.

Hf = activity of the solution from the labeled side at the end of the experiment; Hi = activity of the solution from the labeled side at the beginning of the experiment; K = time constant ($1/\tau$); t = time of the experiment at which we want to calculate the activity in the labeled side. As can be seen from the graph the ratio is stable from around 20 minutes until the end of

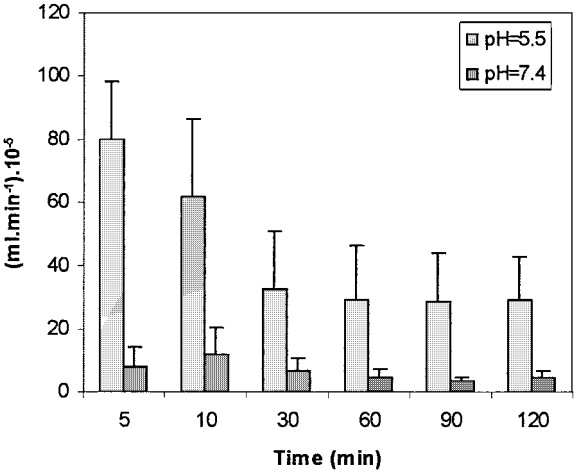

Figure 6. Monitored unidirectional iron flux across mice duodenum measured at pH=7.4 ($n = 3$) and pH=5.5 ($n = 4$). Data are presented as means ± S.E.M. ($p<0.002$).

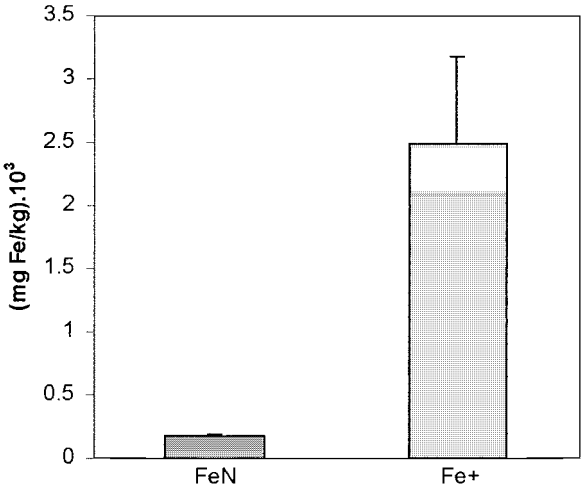

Figure 7. Iron liver concentration (mg/Kg) in parenterally iron loaded B6 mice (Fe+) and controls (FeN). Data are presented as means ± S.E.M., $n = 4$ ($p<0.02$).

the experiment. The first points on the graph probably correspond to the faster isotope release from a liquid layer adherent to the chamber walls after its emptying. To correct for the iron adsorption to the wall chambers and the activity decay of the 'hot' solution during the experiments the radioactivity measured in unlabelled samples was divided by the activity of the labeled side calculated for the respective time period according to the mathematical model described above.

Dependence of iron absorption on pH

In order to determine the influence of the pH on iron movement across duodenal epithelium, unidirectional iron flux measurements were made at pH=7.4 and pH=5.5. The results presented in Figure 6 show that the iron transfer from the apical to the basolateral side of the epithelium is increased in acidic ($n = 4$) compared to neutral pH medium ($n = 3$). Values given correspond to mean ± S.E.M. ($p<0.002$).

Adaptive response of iron absorption to iron loading

Control of the intestinal absorption of iron seems to play an important role in the regulation of iron balance (Flanagan 1989). The capacity to reduce or increase iron absorption in response to increase or reduce iron stores is well documented (O'Riordan *et al.* 1995b; Raja *et al.* 1987; Cox & Peters 1980).

To test whether the *in vitro* method developed could reproduce the results of this adaptive response, unidirectional iron flux measurements were performed

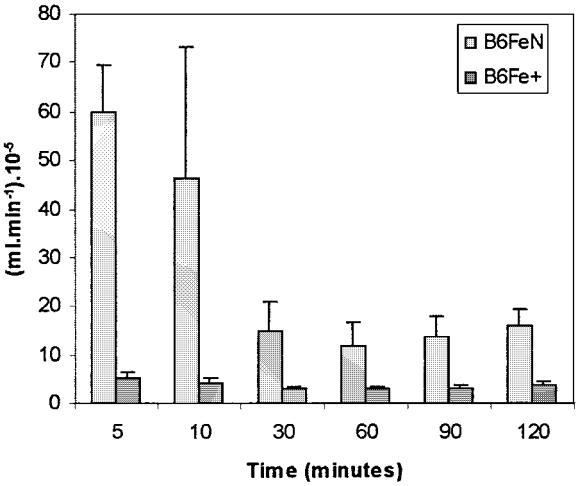

Figure 8. Monitored unidirectional iron flux across duodenal epithelium from iron loaded mice (Fe+, $n = 3$) and mice with normal iron status (FeN, $n = 3$). Data are presented as means ± S.E.M. ($p<0.02$).

in duodenum removed from iron loaded mice. Untreated animals were used as controls for normal iron status. The iron liver concentration (mg Fe/Kg, average±S.E.M.) in animals with different iron status is shown in Figure 7. The results show a significant difference ($p<0.02$) between iron liver concentration in iron loaded mice compared to controls (2485 ± 777 *vs* 180 ± 19, $n = 4$).

As shown in Figure 8 the iron absorption in iron loaded mice was significantly decreased compared to controls ($p<0.02$).

Discussion

Preliminary results from transepithelial electric measurements (Isc, Voc and Gt) in mouse duodenum show that this epithelium in the conditions described is able to generate a spontaneous and stable electrical potential difference that lasts many hours. The measured short-circuit current corresponds to the flow of a positive current in the mucosal-to-serosal direction and seems to be due almost exclusively to a flow of sodium towards the basolateral side. In fact, the current was completely abolished when sodium was replaced bilaterally in the external solutions by NMG whereas the reintroduction of the control solution induced the Isc recovery. The decrease caused on Isc by the addition of ouabain when applied to serosa strongly suggests the presence of the sodium pump in this side of the epithelia. Thus, the flux of sodium through the cell seems to be maintained by the Na^+/K^+-ATPase driving force. In fact, no amiloride sensitive Na^+ channels or Na^+/H^+ co-transport (Gleeson 1992) were detected in the present experiments. In addition, the opposite effects on Isc caused by DIDS (increase of Isc when applied from the serosal side and decrease when applied from the mucosal side) concomitant with the observation of the results obtained with the picrylsulphonic acid (raise on Isc when applied from the serosal side and no effect on Isc when applied from the mucosal side), suggest the presence of a Cl^-/HCO_3^- exchanger Na^+-dependent on the basolateral side of the epithelia. Since DIDS is a known irreversible inhibitor of the Cl^-/HCO_3^- anionic shuttle but also can affect the Na^+-dependent Cl^-/HCO_3^- exchange, the alterations on Isc caused by the use of the picrylsulphonic acid can discriminate between the two transport systems. In this case, the increase in Isc caused by the use of either DIDS or picrylsulphonic acid on the basolateral side of the duodenum suggest the presence of Na^+-dependent Cl^-/HCO_3^- antiport on this side. The suggestion of a Cl^-/HCO_3^- exchanger on the apical side of the epithelium is explained by the fact that DIDS but not picrylsulphonic acid caused Isc alterations when applied from the mucosa. Additionally, the effects on Isc caused by the use of DIDS in the mucosa can probably be explained also by the presence of sensitive-DIDS chloride channels. The decrease observed on Isc when DPC was used on both sides of the epithelium, supports the existence of DPC sensitive-chloride channels on mucosal and basolateral sides. Finally, the observed inefficacy of DIAMOX and Furosemide when applied from both sides of the duodenum rule out a contribution of bicarbonate for the current generation and the existence of a $2Cl^-/Na^+/K^+$ symporter on either side of epithelium, respectively. Taken together, these findings provide some insight into the complexity of the transport systems operating in mouse duodenum.

The study of vectorial iron movement across the duodenum using radionuclide uptake and flux techniques in short circuit conditions proved to be a new and useful method. In fact, the results from the *in vitro* technique described reproduce the adaptive responses to changes in body iron requirements obtained *in vivo*. As expected, a decrease in iron flux across duodenum was observed in samples removed from parenterally iron loaded mice compared to controls. Also, the results from the experiments to test the pH influence on iron movement across duodenal epithelium confirm the increase in iron transfer from the apical to basolateral side of epithelium when the environmental pH varies from neutral to acidic. Finally, a significant difference between Voc measured in duodenum from untreated compared to iron loaded mice was observed suggesting a putative influence of iron loading on transepithelial potential difference. Taken together these results support the use of this Ussing-type model as an alternative *in vitro* method useful to study iron absorption in mouse duodenum. Particularly, the results obtained gain a special interest when trying to understand or evaluate potential-dependent iron transport in the new mouse models available (Fleming *et al.* 1998; Zhou *et al.* 1998; Bahram *et al.* 1999).

Acknowledgements

We are very grateful to Prof. Hugo Gil Ferreira for expert assistance and to Prof. Teresa Moura for the use of the facilities in her laboratory. This study was partially supported by Programa Praxis XXI, Grant BD/5500/95 and Praxis XXI Project 2/2.1/SAU/1323/95.

References

Alvarez-Hernandez X, Nichols GM, Glass J. 1991 Caco-2 cell line: a system for studying intestinal iron transport across epithelial cell monolayers. *Biochim Biophys Acta* **1070**, 205–208.

Bahram S, Gilfillan S, Kühn L *et al.* 1999 Experimental hemochromatosis due to MHC class I HFE deficiency: immune status and iron metabolism. *Proc Nat Acad Sci USA* **96**, 13312–13317.

Cabantchik Z, Greger R. 1992 Chemical probes for anion transporters of mammalian cell membranes. *Am J Physiol* **262**, C803–C827.

Conrad M, Crosby W. 1963 Intestinal Mucosal mechanisms controlling iron absorption. *Blood* **22**, 406–415.

Cox TM, Peters TJ. 1980 Cellular Mechanisms in the regulation of iron absorption by the human intestine: studies in patients with iron deficiency before and after treatment. *Br J Haem* **44**, 75–86.

Crosby WH. 1963 The control of iron balance by the intestinal mucosa. *Blood* **22**, 441–449.

De Sousa M, Reimão R, Lacerda R. *et al.* 1994 Iron overload in β2m-deficient mice. *Immunol Lett* **39**, 105–114.

Edwards JA, Bannerman RM. 1970 Hereditary Defect of Intestinal iron transport in mice with Sex-Linked Anemia. *J Clin Invest* **49**, 1869–1871.

Feder JN, Gnirke A, Thomas W *et al.* 1996 A novel MHC Class I-like gene is mutated in patients with hereditary haemochromatosis. *Nature Genet* **13**, 399–406.

Ferreira HG, Marshall MW. 1985 *The Biophysical Basis of Excitability.* Cambridge: Cambridge University Press.

Ferreira KTG, Fernandes PL, Ferreira HG. 1992 Ion transport across the epithelium of the rabbit caecum. *Biochim Biophys Acta* **1175**, 27–36.

Flanagan PR. 1989 Mechanisms and regulation of intestinal uptake and transfer of iron. *Acta Paediatr Scand Suppl* **361**, 21–30.

Fleming M, Romano MA, Su M *et al.* 1998 Nramp2 is mutated in the anemic Belgrad (b) rat: evidence for a role for Nramp2 in endossomal iron transport. *Proc Nat Acad Sci USA* **95**, 1148–1153.

Fleming, M, Trenor C, Su M *et al.* 1997 Microcytic anaemia mice have a mutation in Nramp2, a candidate iron transporter gene.*Nature Genet* **16**, 383–386.

Gleeson D. 1992 Acid-base transport systems in gastrointestinal epithelia. *Gut* **33**, 1134–1145.

Gunshin H, Mackenzie B, Berger UV *et al.* 1997 Cloning and charactherization of a mammalian proton-coupled metal-ion transporter. *Nature* **388**, 482–488.

Halliday JW. 1992 The regulation of iron absorption: one more piece in the puzzle? *Gastroenterology* **102**, 1071–1079.

Hegel U, Fromm M, Steglitz K. 1993 Bovine and porcine large intestine as model epithelia in a student lab course. *Am J Physiol* **265**, S10–S19.

Madsen KL, Tavernini MM, Mosmann TR, Fedorak RN. 1996 IL-10 modulates ion transport in rat small intestine. *Gastroenterology* **111**, 936–944.

Madshus IH, Olsnes S. 1987 Selective inhibition of sodium linked and sodium independent bicarbonate/chloride antiport in Vero cells. *J Biol Chem* **262**, 7486–7491.

Marvão P, Emílio MG, Ferreira KTG *et al.* 1994 Ion transport in the intestine of *Anguilla Anguilla*: gradients and translocators. *J Exp Biol* **193**, 97–117.

O'Riordan DK, Simpson RJ, Taylor E *et al.* 1995a Hypoxia causes hyperpolarization of isolated rat duodenal brush-border membrane and increased iron absorption. *J Physiol* **489P**, 124P.

O'Riordan PA, Epstein O, Srai SK *et al.* 1995b Rats fed an iron-deficient diet have enhanced intestinal iron transfer and hyperpolarization of the duodenal brush-border membrane. *J Physiol* **482P**, 29P–30P.

Okada Y, Sato T, Inouye A. 1975 Effects of K^+ and Na^+ on membrane potential of epithelial cells in rat duodenum. *Biochim Biophys Acta* **413**, 104–115.

Okada Y, Irimajiri A, Inouye A 1976 Permeability properties and intracellular ion concentration of epithelial cells in rat duodenum. *Biochim Biophys Acta* **436**, 15–24.

Raja K, Bjarnason I, Simpson RJ *et al.* 1987 *In vitro* measurement and adaptative response of Fe^{3+} uptake by mouse intestine. *Cell Biochem Funct* **5**, 69–76.

Raja K, Simpson RJ, Peters T. 1989 Membrane potential dependence of Fe (III) uptake by mouse duodenum. *Biochim Biophys Acta* **984**, 262–266.

Santos M, Schilham MW, Rademakers LHPM *et al.* 1996 Defective iron homeostasis in β2-microglobulin knockout mice recapitulates Hereditary Haemochromatosis in man. *J Exp Med* **184**, 1975–1985.

Schultz SG, Zalusky R. 1964a Ion transport in isolated rabbit ileum: the interaction between active sodium and active sugar transport. *J Gen Physiol* **47**, 567.

Schultz SG, Zalusky R. 1964b Ion transport in isolated rabbit ileum. I. Short-circuit current and Na fluxes. *J Gen Physiol* **47**, 567–584.

Stutts MJ, Henke DC, Boucher RC. 1990 Diphenylamine-2-carboxylate (DPC) inhibits both Cl^- conductance and cyclooxygenase of canine tracheal epithelium. *Pflügers Arch* **415**, 611–616.

Sugawara M, Oikawa H, Kobayashi M *et al.* 1995 Effect of membrane potential on the uptake and the inhibition of cationic compounds in rat intestinal brush-border membrane vesicles and liposomes. *Biochim Biophys Acta* **1234**, 22–28.

Ussing H, Zerahn K. 1951 Active transport of sodium as the source of electric current in the short-circuited isolated frog skin. *Acta Physiol Scand* **23**, 110–127.

Zeuthen T. 1992 From contractile vacuole to leaky epithelia. Coupling between salt and water fluxes in biological membranes. *Biochim Biophys Acta* **1113**, 229–258.

Zhou Y, Tomatsu S, Fleming R *et al.* 1998 HFE gene knockout produces mouse model of hereditary hemochromatosis. *Proc Nat Acad Sci USA* **95**, 2492–2497.